J|A|C|S
ARTICLES
Published on Web 04/22/2005

Molecular Manipulation of Two- and Three-Dimensional Silica Nanostructures by Alkoxysilylation of a Layered Silicate Octosilicate and Subsequent Hydrolysis of Alkoxy Groups

Dai Mochizuki,[†] Atsushi Shimojima,[†] Takeshi Imagawa,[†] and Kazuyuki Kuroda*[,†,‡,§]

Contribution from the Department of Applied Chemistry, Waseda University, Ohkubo-3, Shinjuku-ku, Tokyo 169-8555, Japan, Kagami Memorial Laboratory for Materials Science and Technology, Waseda University, Nishiwaseda-2, Shinjuku-ku, Tokyo 169-0051, Japan, and CREST, Japan Science and Technology Agency (JST), Japan

Received December 28, 2004; E-mail: kuroda@waseda.jp

Abstract: A novel methodology for constructing molecularly ordered silica nanostructures with two-dimensional (2-D) and three-dimensional (3-D) networks has been developed by using a stepwise process involving silylation of a layered silicate octosilicate with alkoxytrichlorosilanes [$ROSiCl_3$, R = alkyl] and subsequent reaction within the interlayer spaces. Alkoxytrichlorosilanes react almost completely with octosilicate, bridging two closest Si−OH (or $-O^-$) sites on the silicate layers, to form new five-membered rings. The unreacted functional groups, Si−Cl and Si−OR, are readily hydrolyzed by the posttreatment with a water/dimethyl sulfoxide (DMSO) or water/acetone mixture, leading to the formation of two types of silicate structures. The treatment with a water/DMSO mixture produced a unique crystalline 2-D silicate framework with geminal silanol groups, whereas a water/acetone mixture induced hydrolysis and subsequent condensation between adjacent layers to form a new 3-D silicate framework. The 2-D structure is retained by the presence of DMSO molecules within the swelled interlayer spaces and is transformed to a 3-D silicate upon desorption of DMSO. The structural modeling suggests that both of the 3-D silicates contain new cagelike frameworks where solvent molecules are trapped even at high temperature (up to 380 °C, in the case of acetone). Both 2-D and 3-D silica structures are quite different from known layered silicates and zeolite-like materials, indicating the potential of the present approach for precise design of various silicate structures at the molecular level.

Introduction

Ordered silica structures have received broad interest in basic chemistry and applications, including catalysis and adsorption.[1] The precise design of both silica frameworks and nanospaces created by those networks is a critical issue. Although hydrothermal synthesis has been adopted to construct crystalline silica frameworks such as zeolites and layered silicates, the capability to control the frameworks is limited.[2] Recently, surfactants are widely used as a structural director for fabricating mesoscopically ordered silica under mild conditions.[3,4] However, such materials have amorphous silica frameworks, and the crystal-like ordering of the frameworks has been achieved only by the posttreatment under hydrothermal conditions.[4,5] It remains a challenge to establish a versatile and soft-chemical methodology for designing ordered silica structures at the molecular scale.

Layered silicates and aluminosilicates with two-dimensional (2-D) crystalline structures are important for their ability to accommodate various molecules within the interlayer spaces.[6,7] Furthermore, they are useful as scaffolds for the construction of three-dimensional (3-D) silicate materials. Pinnavaia et al. reported the pillaring of the interlayer spaces of a layered silicate by condensation of silicic acids in the presence of the surfactant to form a porous clay heterostructure (PCH).[8] We have reported the formation of mesoporous silica (KSW-2) by winding the silicate layers of kanemite through the interactions with sur-

[†] Department of Applied Chemistry, Waseda University.
[‡] Kagami Memorial Laboratory for Materials Science and Technology, Waseda University.
[§] CREST.

(1) (a) Davis, M. E. *Nature* **1996**, *382*, 583−585. (b) Davis, M. E. *Nature* **2002**, *417*, 813−821.
(2) (a) Barrer, R. M. *Hydrothermal Chemistry of Zeolites*; Academic Press: London, 1982. (b) Lagaly, G. *Adv. Colloid Interface Sci.* **1979**, *11*, 105−148. (c) Cundy, C. S.; Cox, P. A. *Chem. Rev.* **2003**, *103*, 663−701.
(3) Ying, J. Y.; Mehnert, C. P.; Wong, M. S. *Angew. Chem., Int. Ed.* **1999**, *38*, 56−77.
(4) (a) Christiansen, S. C.; Zhao, D.; Janicke, M. T.; Landry, C. C.; Stucky, G. D.; Chmelka, B. F. *J. Am. Chem. Soc.* **2001**, *123*, 4519−4529. (b) Hedin, N.; Graf, R.; Christiansen, S. C.; Gervais, C.; Hayward, R. C.; Eckert, J.; Chmelka, B. F. *J. Am. Chem. Soc.* **2004**, *126*, 9425−9432.
(5) (a) Khushalani, D.; Kuperman, A.; Ozin, G. A.; Tanaka, K.; Garces, J.; Olken, M. M.; Coombs, N. *Adv. Mater.* **1995**, *7*, 842−846. (b) Sayari, A.; Liu, P.; Kruk, M.; Jaroniec, M. *Chem. Mater.* **1997**, *9*, 2499−2506. (c) Chen, L. Y.; Horiuchi, T.; Mori, T.; Maeda, K. *J. Phys. Chem. B* **1999**, *103*, 1216−1222.
(6) (a) Corma, A. *Chem. Rev.* **1997**, *97*, 2373−2419. (b) Occelli, M. L. *Catal. Today* **1988**, *2*, 339−355. (c) Ogawa, M.; Kuroda, K. *Bull. Chem. Soc. Jpn.* **1997**, *70*, 2593−2618. (d) Auerbach, S. M.; Carrado, K. A.; Dutta, P. K. *Handbook of Layered Materials*; Mercel Dekker: New York, 2004.
(7) (a) Corma, A.; Fornes, V.; Pergher, S. B.; Maesen, T. L. M.; Buglass, J. G. *Nature* **1998**, *396*, 353−356. (b) Corma, A.; Fornes, V.; Guil, J. M.; Pergher, S.; Maesen, T. L. M.; Buglass, J. G. *Microporous Mesoporous Mater.* **2000**, *38*, 301−309.
(8) (a) Tanev, P. T.; Pinnavaia, T. J. *Science* **1996**, *271*, 1267−1269. (b) Choy, J. H.; Jung, H.; Han, Y. S.; Yoon, J. B.; Shul, Y. G.; Kim, H. J. *Chem. Mater.* **2002**, *14*, 3823−3828.

factants.[9] However, the silicate structure of the product does not completely reflect the original structure. Recently the 3-D zeolite structures (CDS-1, ERS-12, MCM-65, MCM-69, Nu-6, and RUB-41) were synthesized through the topotactic conversion of 2-D precursors by careful calcination.[10] Also, a new type of silica zeolite (RUB-24) containing 8MR was synthesized from intercalated octosilicate by the condensation of the silicate layers during calcination.[11] This method can serve as a promising route to produce a 3-D structure that reflects the crystallinity of the original layered structures, but basically imposes a limitation on the use of other layered silicate because of difficulty in the connection of Si−OH groups between adjacent layers.

A new approach proposed here is to manipulate silica frameworks based on a stepwise reaction of monomeric Si species within the interlayer spaces of layered silicates.[12] Silylation of the surface silanol groups of layered silicates with organochlorosilanes has been utilized to prepare a variety of layered silica−organic nanomaterials.[13] We reported the formation of new ring structures on the silicate layers by silylation of kanemite with alkylchlorosilanes.[13e] However, the single silicate sheets of kanemite deteriorated upon silylation. Our interest has therefore been focused on layered octosilicate[14] (also known as ilerite[14a] or RUB-18[14c]), which has a more rigid structure consisting of four-, five-, and six-membered rings (abbreviated as 4MR, 5MR, and 6MR, respectively) and Si−OH/Si−O$^-$ groups on its surface. By using dialkoxydichlorosilanes [$(RO)_2SiCl_2$, R = alkyl] as silylating agents, we obtained a unique crystalline 2-D silica structure where dialkoxysilyl groups are regularly grafted on the silicate layers to form new 5MR.[15] The products are potentially applicable as precursors for new silica-based nanomaterials either by exchanging alkoxy groups or by hydrolysis and condensation.[16] However, the dialkoxy groups on the interlayer surfaces remained intact even when the products were dispersed in an aqueous or alcoholic solution under acidic conditions. It appears that highly hydrophobic interlayer spaces consisting of bilayers of alkoxy groups blocked the intercalation of water molecules to hydrolyze Si−OR groups.

In this paper, we report the formation of novel silica structures by silylation of octosilicate with alkoxytrichlorosilanes [$ROSiCl_3$]. By controlling the reaction conditions, two Si−Cl groups of an alkoxytrichlorosilane molecule react with two silanol groups on a silicate layer to form new 5MR. Importantly, the silylated product is bifunctional having both Si−Cl and Si−OR groups. Although Si−Cl group is useful for various reactions,[17] we focus on its role as "trigger" for hydrolysis of the alkoxy groups. The high reactivity of Si−Cl group with water leads to the formation of Si−OH and HCl; the former creates less hydrophobic interfaces for further intercalation of water molecules, and the latter catalyzes the hydrolysis of alkoxy groups.[16] As a result, we succeeded in the fabrication of novel crystalline 2D silica with geminal silanol groups. Moreover, a 3-D silica structure with 12MR was formed by condensation between the silanol groups on adjacent layers. Such a route opens a new possibility to create unique 2-D and 3-D silica structures that are not accessible by conventional methods.

Experimental Section

Synthesis of Na−Octosilicate and C_{16}TMA−Octosilicate. Na−octosilicate (Na−Oct; $Na_8[Si_{32}O_{64}(OH)_8 \cdot 32H_2O]$) was synthesized by the method reported previously.[18] SiO_2 (special grade, Wako Chemicals), NaOH, and distilled water were mixed at a ratio of SiO_2:Na_2O:H_2O = 4:1:25.8. The mixture was treated at 100 °C for 2 weeks in a sealed Teflon vessel. Hexadecyltrimethylammonium−octosilicate (C_{16}TMA−Oct) was prepared by the ion exchange reaction of Na−Oct with hexadecyltrimethylammonium chloride [$C_{16}H_{33}N(CH_3)_3Cl$, C_{16}TMACl] (Tokyo Kasei Co.).[18] Na−Oct (12 g) was dispersed in an aqueous solution of C_{16}TMACl (0.1 mol/L, 400 mL). The mixture was stirred at room temperature for 24 h and then centrifuged to remove the supernatant. This procedure was repeated three times. The resulting slurry was washed with water and air-dried at room temperature.

Synthesis of Alkoxytrichlorosilanes. Alkoxyltrichlorosilanes [$(C_nH_{2n+1}O)SiCl_3$; **1(C$_n$)** (Scheme 1), n = 6, 8, 10, and 12] were synthesized by a similar method for dialkoxydichlorosilane.[15] In a typical procedure, *n*-alcohol (C*n*OH, n = 6, 8, 10, or 12, Tokyo Kasei Co.) was added dropwise to a vigorously stirred mixture of $SiCl_4$ (Tokyo Kasei Co.) and hexane ($SiCl_4$/C*n*OH = 1) under an N_2 flow. The mixture was allowed to react at room temperature for 1 h, yielding the mixture of $(CnO)_mSiCl_{4-m}$ (m = 0−4). Alkoxytrichlorosilanes (m = 1) were separated by distillation (0.1 Torr, bp; ∼50 °C (n = 6), ∼70 °C (n = 8), ∼90 °C (n = 10), and ∼110 °C (n = 12)). The ^{29}Si NMR spectrum of **1(C$_{12}$)**, for example, exhibited a single signal at −38.5 ppm assignable to (C*n*O)*Si*Cl_3 (Figure S1A).[19] In addition, the ^{13}C NMR spectrum showed the signals assigned to the alkoxy groups (Figure S1B), where the signal of α carbon (SiO*C*) appeared at 66.6 ppm, being shifted from that of dodecyl alcohol (62.5 ppm). The ^{13}C and ^{29}Si NMR spectra for other **1(C$_n$)** (n = 6, 8, and 10) also confirmed the formation of these reagents (Figure S1).

Silylation. C_{16}TMA−Oct (1.5 g) dispersed in dehydrated dichloromethane (30 mL) and dehydrated pyridine (10 mL) was mixed with an excess (20 mmol) of alkoxytrichlorosilane **1(C$_n$)**. The mixture was

(9) Kimura, T.; Kamata, T.; Fuziwara, M.; Takano, Y.; Kaneda, M.; Sakamoto, Y.; Terasaki, O.; Sugahara, Y.; Kuroda, K. *Angew. Chem., Int. Ed*. **2000**, *39*, 3855−3859.

(10) (a) Ikeda, T.; Akiyama, Y.; Oumi, Y.; Kawai, A.; Mizukami, F. *Angew. Chem., Int. Ed.* **2004**, *43*, 4892−4896. (b) Millini, R.; Carluccio, L. C.; Carati, A.; Bellussi, G.; Perego, C.; Cruciani, G.; Zanardi, S. *Microporous Mesoporous Mater*. **2004**, *74*, 59−71. (c) Dorset, D. L.; Kennedy, G. J. *J. Phys. Chem. B* **2004**, *108*, 15216−15222. (d) Rollmann, L. D.; Schlenker, J. L.; Lawton, S. L.; Kennedy, C. L.; Kennedy, G. J. *Microporous Mesoporous Mater*. **2002**, *53*, 179−193. (e) Schreyeck, L.; Caullet, P.; Mougenel, J. C.; Guth, J. L.; Marler, B. *Microporous Mater*. **1996**, *6*, 259−271. (f) Zanardi, S.; Alberti, A.; Cruciani, G.; Corma, A.; Fornés, V.; Brunelli, M. *Angew. Chem., Int. Ed.* **2004**, *43*, 4933−4937. (g) Wang, Y. X.; Gies, H.; Marler, B.; Muller, U. *Chem. Mater*. **2005**, *17*, 43−49.

(11) Marler, B.; Stöter, N.; Gies, H. *Recent Research Reports of the 14th International Zeolite Conference* **2004**, 15−16.

(12) (a) Beneke, K.; Lagaly, G. *Am. Mineral*. **1977**, *62*, 763. (b) Eugster, H. P. *Science* **1967**, *157*, 1177−1180.

(13) (a) Ruiz-Hitzky, E.; Rojo, J. M. *Nature* **1980**, *287*, 28−30. (b) Ruiz-Hitzky, E.; Rojo, J. M.; Lagaly, G. *Colloid Polym. Sci.* **1985**, *263*, 1025−1030. (c) Yanagisawa, T.; Kuroda, K.; Kato, C. *React. Solids* **1988**, *5*, 167−175. (d) Ogawa, M.; Okutomo, S.; Kuroda, K. *J. Am. Chem. Soc*. **1998**, *120*, 7361−7362. (e) Shimojima, A.; Mochizuki, D.; Kuroda, K. *Chem. Mater*. **2001**, *13*, 3603−3609. (f) Fujita, I.; Kuroda, K.; Ogawa, M. *Chem. Mater*. **2003**, *15*, 3134−3141.

(14) (a) Iler, R. K. *J. Colloid Sci*. **1964**, *19*, 648−657. (b) Schwieger, W.; Heidemann, D.; Bergk, K. H. *Rev. Chim. Miner*. **1985**, *22*, 639−650. (c) Vortmann, S.; Rius, J.; Siegmann, S.; Gies, H. *J. Phys. Chem. B* **1997**, *101*, 1292−1297. (d) Huang, Y.; Jiang, Z.; Schwieger, W. *Chem. Mater*. **1999**, *11*, 1210−1217. (e) Brenn, U.; Ernst, H.; Freude, D.; Herrmann, R.; Jähnig, R.; Karge, H. G.; Kärger, J.; König, T.; Mädler, B.; Pingel, U. T.; Prochnow, D.; Schwieger, W. *Microporous Mesoporous Mater*. **2000**, *40*, 43−52. (f) Wolf, I.; Gies, H.; Fyfe, C. A. *J. Phys. Chem. B* **1999**, *103*, 5933−5938. (g) Borowski, M.; Wolf, I.; Gies, H. *Chem. Mater*. **2002**, *14*, 38−43.

(15) Mochizuki, D.; Shimojima, A.; Kuroda, K. *J. Am. Chem. Soc*. **2002**, *124*, 12082−12083.

(16) Brinker, C. J.; Scherer, G. W. *Sol−Gel Science*; Academic Press: San Diego, CA, 1990.

(17) Giesenberg, T.; Hein, S.; Binnewies, M.; Kickelbick, G. *Angew. Chem., Int. Ed*. **2004**, *43*, 5697−5700.

(18) Endo, K.; Sugahara, Y.; Kuroda, K. *Bull. Chem. Soc. Jpn.* **1994**, *67*, 3352−3355.

(19) Liepins, E.; Zicmane, I.; Lukevics, E. *J. Organomet. Chem.* **1986**, *306*, 167−182.

Scheme 1. Silylation of Octosilicate by Alkoxytrichlorosilane and Hydrolysis of the Silylated Product

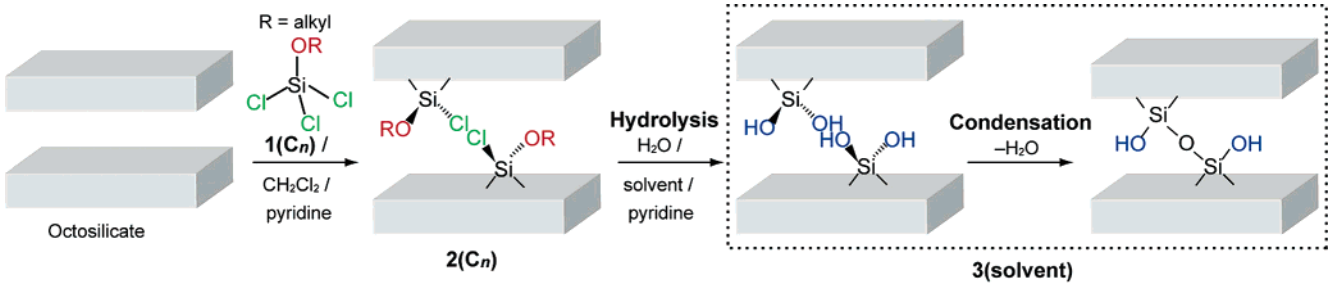

stirred at room temperature for 1 day under N_2 atmosphere. The solid products were filtered and washed with dichloromethane to remove unreacted silylating reagents, pyridine hydrochloride, and deintercalated C_{16}TMACl. The resulting products were dried in vacuo to yield **2(C$_n$)** (Scheme 1). They were stored in N_2 atmosphere to avoid hydrolysis of the interlayer Si−Cl and Si−OR groups.

Alcoholysis. The silylated-derivative **2(C$_{12}$)** (0.25 g) was stirred in a mixture of dodecyl alcohol (2.0 g), toluene (10 mL), and pyridine (1.0 mL) for 1 day. The product was filtered, washed with toluene, and dried in vacuo.

Hydrolysis of Alkoxy Groups with Water/(DMSO or Acetone). **2(C$_{12}$)** (0.5 g) was added to a mixture of DMSO (40 mL) (or acetone), H_2O (10 mL), and pyridine (1.0 mL).[20] After being stirred for 1 day, the mixture was centrifuged, and the solid components were washed with a mixture of the solvent (DMSO or acetone) and water. The products after drying in vacuo for 2 h are designated as **3(DMSO)** and **3(acetone)** (Scheme 1).

Analysis. Powder X-ray diffraction (XRD) measurements were performed on a Rigaku Rint 2000 powder diffractometer with a radiation of Ni-filtered Cu Kα (λ = 0.15418 nm). Thermogravimetry (TG) was carried out with a Rigaku Thermo Plus2 instrument under a dry air flow at a heating rate of 10 °C min^{-1}, and the amounts of SiO_2 fractions in the products were determined by the residual weight after heating to 900 °C. The amounts of organic constituents were determined by CHN analysis (Perkin-Elmer PE-2400). Solid-state ^{29}Si MAS NMR spectra were recorded on a JEOL JNM-CMX-400 spectrometer at a resonance frequency of 79.42 MHz with a 45° pulse and a recycle delay of 200 s. The samples were put into 7.5 mm (or 5 mm) zirconia rotors and spun at 5 kHz. We confirmed that the signals were fully relaxed under these conditions so that quantitative analysis was possible. Solid-state ^{13}C CP/MAS NMR spectra were recorded on the same spectrometer at a resonance frequency of 100.40 MHz and a recycle delay of 5 s. The ^{29}Si and ^{13}C chemical shifts were referenced to tetramethylsilane at 0 ppm. TG-MS (mass spectrometry) analysis was performed on a combined Rigaku Thermo Plus2 and GCMS-QP1100EX under He atmosphere at a heating rate of 20 °C min^{-1}. The structurally optimized calculation was performed with an Accelrys Discover software by using the COMPASS force field. The scanning electron microscopy (SEM) images were obtained with a JEOL JSM-5500LV microscope at an accelerating voltage of 25 kV.

Results

Silylation of Octosilicate with Alkoxytrichlorosilanes (1(C$_n$)). The XRD patterns of Na−Oct, C_{16}TMA−Oct, and **2(C$_{12}$)** are shown in Figure 1a−c, respectively. The pattern of **2(C$_{12}$)** is quite different from those of C_{16}TMA−Oct and Na−Oct and exhibits a peak in the small angle region with a *d* spacing of 2.05 nm. The *d* spacing of **2(C$_n$)** increases linearly with the increase in the carbon number (*n*) of the silylating agents (**1(C$_n$)**) used (Figure S2, inset), suggesting that alkoxysilyl groups are introduced into the interlayer spaces. The higher 2θ region in the pattern of **2(C$_{12}$)** (Figure 1c) displays

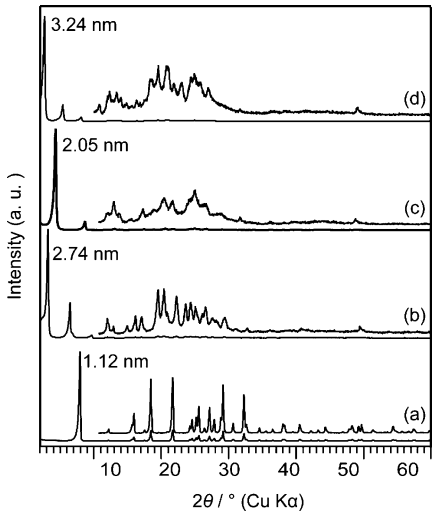

Figure 1. XRD patterns of (a) Na−Oct, (b) C_{16}TMA−Oct, (c) **2(C$_{12}$)**, and (d) **2(C$_{12}$)** treated with dodecyl alcohol.

many peaks due to a well-defined framework structure. The lattice constant of the *a*-axis (a = 0.743 nm) is slightly larger than that of Na−Oct (a = 0.733 nm), which might be caused by the distortion of the silicate framework by silylation. Although the space group symmetry should be lowered, as suggested by broadened XRD peaks and ^{29}Si NMR signals (shown below), all of the diffraction peaks can be assigned to a tetragonal cell (space group $I4_1/amd$), the same group as that of Na−Oct, using the lattice parameters of a = 0.743 nm and c = 8.20 nm.

The complete removal of C_{16}TMA ions upon silylation was confirmed by the absence of nitrogen in **2(C$_{12}$)**, while the nitrogen content in C_{16}TMA−Oct was 2.4% (Table 1), implying

Table 1. Amounts of Alkoxy Groups of the Products

	mass %C	mass %H	mass %N	%SiO_2	amount of alkoxy groups /(SiOH + SiO^-)[a]
C_{16}TMA−Oct	39.3	8.4	2.4	49.8	
2(C$_{12}$)	27.8	5.2	0.0	59.9	0.49
2(C$_{12}$) treated with dodecyl alcohol	40.6	7.2	0.0	48.1	1.04
3(DMSO)	22.8	4.8	0.0	58.3	
3(acetone)	7.1	1.4	0.2	89.3	

[a] Evaluated by CHN analysis and thermogravimetry.

that all of the carbon (27.8 wt %) originated from the alkoxy groups of **1(C$_n$)**. Actually, the ^{13}C CP/MAS NMR spectrum of

(20) When the reaction was performed without pyridine, the alkoxy groups were not hydrolyzed completely.

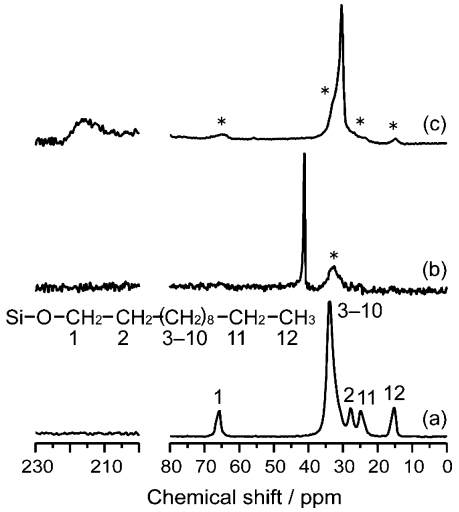

Figure 2. ^{13}C CP/MAS NMR spectra of (a) **2(C$_{12}$)**, (b) **2(DMSO)**, and (c) **3(acetone)**.

2(C$_{12}$) exclusively exhibits the signals corresponding to dodecoxy groups (Figure 2a). The chemical shift of α carbon of alkyl alcohols is reported to depend on the state; the shifts are 63 ppm for those physically adsorbed on silica surface and 64.5−65 ppm for those forming Si−O−C linkage.[21] The appearance of a single signal at 65 ppm in Figure 2a strongly indicates the presence of dodecoxysilyl groups without the cleavage of Si−O−C linkage. Other silylated derivatives (**2(C$_n$)**; n = 6, 8, and 10) also show the signals at 65 ppm due to the alkoxysilyl groups (Figure S3A).

The ^{13}C signal of interior methylene carbons appearing at 33 ppm (Figure 2a) indicates that the chains adopt all-trans conformations.[22] No signal was observed at around 30 ppm indicative of chains containing gauche defects,[22] which is in clear contrast to dialkoxysilylated octosilicate.[15] In addition, the average increment of the d spacings per one CH_2 groups in **2(C$_n$)** (ca. 0.10 nm/CH_2, Figure S2, inset) is about one-half of the value for dialkoxysilylated octosilicates having bilayer arrangements of alkoxy groups (ca. 0.19 nm/CH_2).[15] This value suggests that the alkoxy groups in **2(C$_n$)** are arranged in an interdigitated monolayer with a slight inclination of the chain axis normal to the silicate layers.

The information about the siloxane frameworks was obtained by ^{29}Si MAS NMR spectra (Figure 3). The spectrum of C_{16}TMA−Oct (Figure 3a) shows two narrow signals at −100 and −110 ppm corresponding to the Q^3 ($Si(OSi)_3(O^-)$) and Q^4 ($Si(OSi)_4$) units, respectively. The intensity ratio of these signals is 1:1 (Q^3/Q^4 = 1) (Table 2). As shown in the spectrum of **2(C$_{12}$)** (Figure 3b), the silylation resulted in the significant decrease of the Q^3 signal (Q^3/Q^4 = ∼0.03), while a new signal was observed at around −84 ppm. This new signal can be ascribed to grafted alkoxysilyl groups ($Si(OSi)_2Cl(OR)$, designated as the I site). The shoulder signal at −86 ppm suggests the presence of the I site with a different bonding state,[13e] but its relative intensity is very small (∼11%). The significant downfield shift of the I site as compared to the Q^2 signals of silica, which typically appear between −90 to −96 ppm,[16] can be ascribed

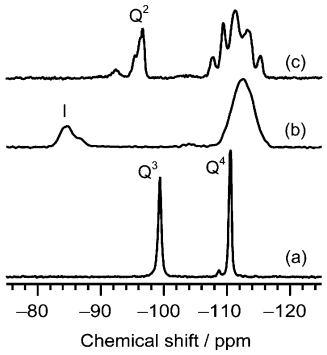

Figure 3. ^{29}Si MAS NMR spectra of (a) C_{16}TMA−Oct, (b) **2(C$_{12}$)**, and (c) **2(C$_{12}$)** treated with dodecyl alcohol.

Table 2. Relative Intensity in the ^{29}Si MAS NMR Spectra for the Products

	I	Q^2	Q^3	Q^4	$(Q^4-1)/I^c$
C_{16}TMA−Oct			1.00	1.00	
2(C$_{12}$)[a]	0.45		0.05	1.95	2.1
3(DMSO)[b]		0.44	0.08	1.93	
3(acetone)[b]		0.07	0.47	1.91	

[a] Relative intensities of **2(C$_{12}$)** were normalized as a total Q^3 and Q^4 area to be 2.0 for the comparison to that of C_{16}TMA−Oct. [b] Relative intensities of **3(DMSO)** and **3(acetone)** were normalized as a total spectral area to be 2.45 for the comparison to that of **2(C$_{12}$)**. [c] (Q^4 − 1) means new Q^4 sites created by silylation.

to the presence of a Si−Cl bond. Although such a downfield shift of ^{29}Si signal has been observed for SiO_4 units forming 3MR,[23] it is apparent that 3MR are not contained in **2(C$_{12}$)**. The formation of 3MR by silylation should lead to the appearance of two downfield signals with the intensity ratio of 1:2 that corresponds to the grafted silyl groups and newly formed Q^4 units on octosilicate, respectively. Figure 3b mainly shows one downfield signal (−84 ppm), suggesting that the signal is due to the alkoxysilyl groups. The relative intensity of this signal is 0.45 per one Si−OH (or $-O^-$) group (Q^3) of octosilicate, which is in good agreement with the number of attached alkoxysilyl groups (0.49) per Si−OH (or $-O^-$) evaluated by TG and elemental analysis. The relative intensity of the Q^3 signal of C_{16}TMA−Oct decreased to ca. 0.1 after silylation, indicating that about 90% of the reactive sites are silylated. In addition, the increase of the Q^4 signal with respect to the I signal ($(Q^4-1)/I$) is 2.1, which indicates that one alkoxytrichlorosilane molecule reacted with two silanols of octosilicate. Similar results were also obtained for **2(C$_n$)** (n = 6, 8, and 10) (Figure S3B and Table S1). The structural model is depicted in Scheme 2B.

Alcoholysis of Silylated Derivative 2(C$_{12}$). To confirm the reactivity of the Si−Cl groups, **2(C$_{12}$)** was treated with dodecyl alcohol. The d spacing increased from 2.05 to 3.24 nm (Figure 1d), and the major XRD peaks roughly matched the pattern of didodecoxysilylated octosilicate reported previously.[15] In addition, the amount of carbon per 1 SiO_2 became almost twice as large as that of **2(C$_{12}$)** (Table 1). The ^{29}Si MAS NMR spectrum (Figure 3c) shows a new signal at −96 ppm assigned to dialkoxysilyl groups (Q^2), the relative intensity of which is consistent with that of the I site observed in Figure 3b. The small signal at −93 ppm is assigned to the Q^2 units [$Si(OSi)_2$-(OH)(OR)] formed by the hydrolysis of Si−Cl groups during

(21) Ossenkamp, G. C.; Kemmitt, T.; Johnston, J. H. *Chem. Mater.* **2001**, *13*, 3975−3980.
(22) (a) Gao, W.; Reven, L. *Langmuir* **1995**, *11*, 1860−1863. (b) Gao, W.; Dickinson, L.; Grozinger, C.; Morin, F. G.; Reven, L. *Langmuir* **1997**, *13*, 115−118.
(23) (a) Rohrig, C.; Gies, H. *Angew. Chem., Int. Ed. Engl.* **1995**, *34*, 63−65. (b) McCusker, L. B.; Grosse-Kunstleve, R. W.; Baerlocher, C.; Yoshikawa, M.; Davis, M. E. *Microporous Mater.* **1996**, *6*, 295−309.

Scheme 2. (A) Silicate Crystal Structure of Octosilicate (left) Viewed along the *b* Axis, and (right) Viewed along the *c* Axis; (B) Proposed Structural Model of **2(C*n*)** (left) Viewed along the *b* Axis, and (right) Viewed along the *c* Axis

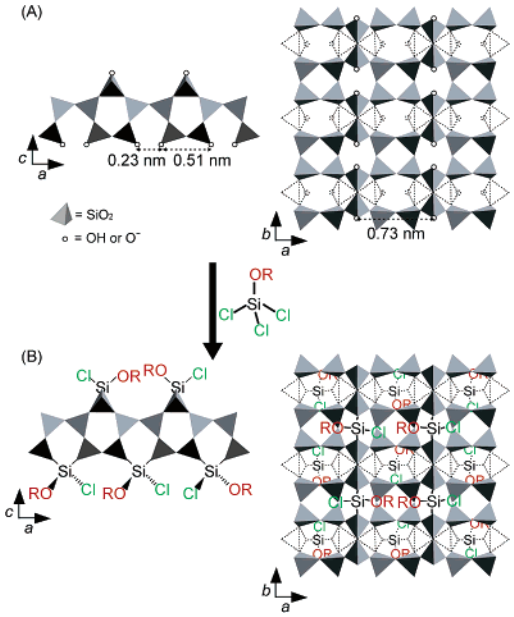

the reaction. The split of the Q^4 signals into −108, −110, −112, −114, and −115 ppm is also observed for dialkoxysilylated octosilicate.[15] This split appears to be inherent to the silicate framework of octosilicate, although the detail is unclear.[14e] These data clearly show the formation of dialkoxysilyl groups by the reaction with alcohols, implying that the interlayer Si−Cl groups in **2(C$_{12}$)** have high reactivity and accessibility.

Hydrolysis of Silylated Derivatives 2(C$_n$). Figure 4 shows the XRD patterns of **2(C$_{12}$)** after the treatment with the mixtures of water and solvent (DMSO or acetone). The *d* values decrease to 1.66 and 1.12 nm for **3(DMSO)** and **3(acetone)**, respectively. Also, these patterns display different profiles in the higher angle region (2θ = 10°−60°), but show the same peaks at 49° corresponding to the lattice constant of the *a*-axis in Na−Oct. Although the quality of XRD pattern decreased upon hydrolysis, the presence of several peaks at higher 2θ region indicates that the products still retain well-defined framework structures. The SEM images of C16TMA-Oct, **2(C$_{12}$)**, **3(DMSO)**, and **3(acetone)** (Figure 5) reveal that the particle size (ca. 2−10 μm) and the square-shaped morphology of octosilicate are preserved during the silylation and hydrolysis processes.

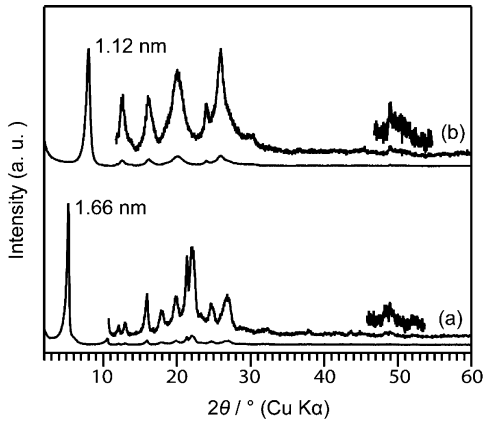

Figure 4. XRD patterns of (a) **3(DMSO)** and (b) **3(acetone)**.

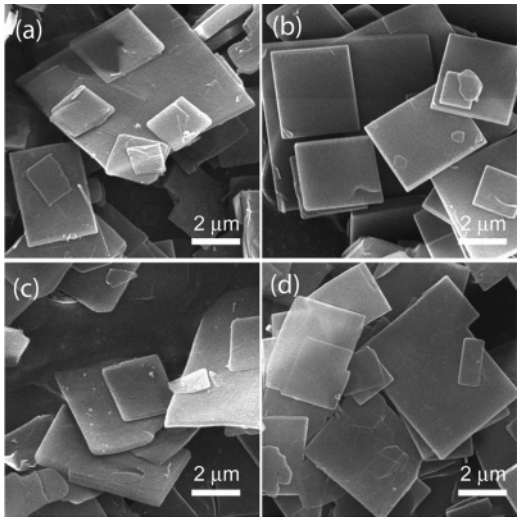

Figure 5. SEM images of (a) C_{16}TMA−Oct, (b) **2(C$_{12}$)**, (c) **3(DMSO)**, and (d) **3(acetone)**.

The carbon contents in **3(DMSO)** and **3(acetone)** are 23 and 7 wt %, respectively, being smaller than that of **2(C$_{12}$)** (28 wt %) (Table 1). The ^{13}C CP/MAS NMR spectra (Figure 2b and 2c) revealed the significant decrease in the signal of the alkoxy groups (∗), indicating the hydrolysis of the interlayer alkoxy groups. These spectra also show the signals due to DMSO (40 ppm, S−*C*H$_3$) and acetone (30 ppm, *C*H$_3$; 215 ppm, *C*═O). It is reported that the acidity of zeolite can be evaluated by the ^{13}C chemical shift of carbonyl carbon of acetone molecules adsorbed on its surface.[24] In Figure 2c, the signal of the carbonyl carbon is shifted downfield (215 ppm) from that in solution (206 ppm), suggesting the weak acidity of **3(acetone)** similar to formic acid.

The FT-IR spectra of **3(DMSO)** and **3(acetone)** (Figure S4A) show broad O−H stretching vibrations centered at 3440 cm^{-1} ascribed to the silanol groups hydrogen-bonded to solvent or water. In addition, in the case of **3(acetone)**, the C═O stretching vibration bands of acetone are observed at 1690 cm^{-1} with a shoulder at 1705 cm^{-1}. These two bands can be ascribed to the interaction between one carbonyl group and one Si−OH group, and that between one carbonyl group and two Si−OH groups, respectively.[25] On the other hand, the hydrogen bond between DMSO and the silanol groups in **3(DMSO)** was evidenced by the Raman spectrum (Figure S4B), which shows the S═O stretching vibration at 1022 cm^{-1}.[26]

Figure 6 shows the ^{29}Si MAS NMR spectra of the hydrolyzed products. The signal corresponding to the *Si*Cl(OR) groups (−84 ppm) was not observed in both spectra. The spectrum of **3(DMSO)** shows a new signal at −91 ppm, which is attributed to the Q^2 units possessing geminal silanol groups [(SiO)$_2$*Si*(OH)$_2$],[16] along with the Q^4 signal (−112 ppm). On the other hand, **3(acetone)** mainly shows broad signals due to the Q^3 (−101 ppm) and Q^4 units, and a very small signal was observed in the Q^2 region. As listed in Table 2, the relative intensities of these new Q^2 and Q^3 signals (in Figure 6a and b,

(24) Barich, D. H.; Nicholas, J. B.; Xu, T.; Haw, J. F. *J. Am. Chem. Soc.* **1998**, *120*, 12342−12350.
(25) (a) Storozheva, E. N.; Tsyganenko, A. A. *Russ. J. Phys. Chem.* **2003**, *77*, 458−461. (b) Okunev, A. G.; Paukshtis, E. A.; Aristov, Y. I. *React. Kinet. Catal. Lett.* **1998**, *65*, 161−167.
(26) Johnston, C. T.; Sposito, G.; Bocian, D. F.; Birge, R. R. *J. Phys. Chem.* **1984**, *88*, 5959−5964.

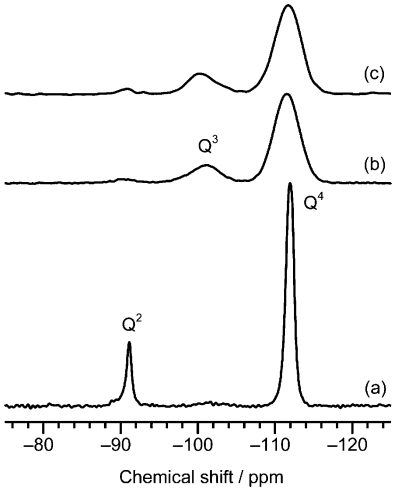

Figure 6. ^{29}Si MAS NMR spectra of (a) **3(DMSO)**, (b) **3(acetone)**, and (c) **3(DMSO)** vacuum-dried for 48 h.

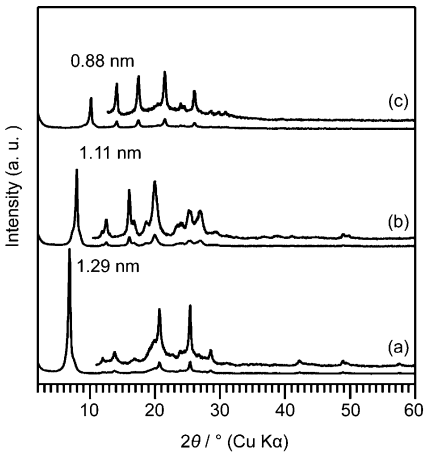

Figure 7. XRD patterns of **3(DMSO)** dried in vacuo for (a) 48 h and (b) 100 h, and (c) the product calcined at 550 °C.

respectively) are approximately equal to that of the *I* signal of **2(C$_{12}$)**. In addition, the relative intensities of the Q^4 site were almost unchanged before and after hydrolysis. These results indicate that the alkoxychlorosilyl groups in **2(C$_{12}$)** were mostly transformed to new Q^2 and Q^3 sites for **3(DMSO)** and **3(acetone)**, respectively.

Desorption of Adsorbed Molecules from Hydrolyzed Products. The structural transformation of **3(DMSO)** induced by desorption of DMSO was demonstrated by XRD (Figure 7). As described above, **3(DMSO)** was obtained by drying in vacuo for 2 h after hydrolysis, and exhibits the basal spacing of $d = 1.66$ nm (Figure 4a). When the drying-time was extended to 48 h, the *d* value of the sample decreased to 1.29 nm (Figure 7a). The ^{29}Si MAS NMR spectrum of the sample dried for 48 h revealed that the decrease of the basal spacing is accompanied by the condensation between the Q^2 units to form the Q^3 units (Figure 6c). The XRD pattern of the product dried for 100 h is 1.11 nm (Figure 7b). The profiles of both XRD pattern and ^{29}Si MAS NMR spectrum are very similar to those of **3(acetone)**, suggesting the formation of 3-D frameworks similar to **3(acetone)**. After the complete removal of organic species by heating at 550 °C, **3(DMSO)** still retains the ordered structure with the *d* value of 0.88 nm (Figure 7c).

The thermal behavior of the hydrolyzed products is also investigated. The TG curve for **3(DMSO)** (dried for 2 h) and

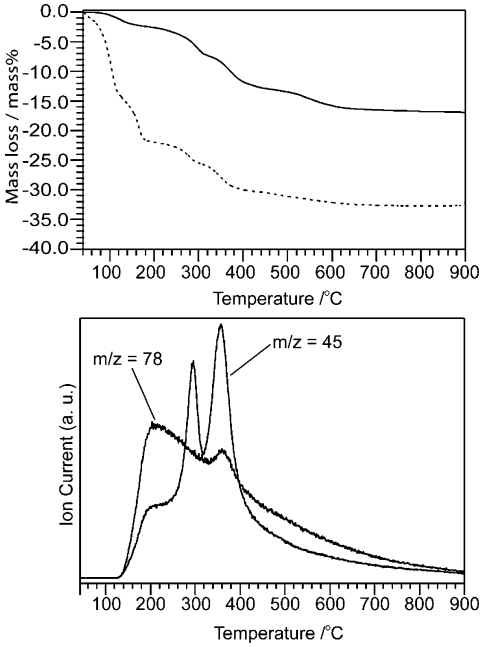

Figure 8. (Top) Thermogravimetric curves of **3(DMSO)** after drying in vacuo for 2 h (dotted line) and 48 h (solid line). (Bottom) Mass spectrometric analysis of **3(DMSO)** dried for 48 h. The mass fragments correspond to molecular fragment ($m/z = 78$) of DMSO and the $[HCS]^+$ ($m/z = 45$) fragment.

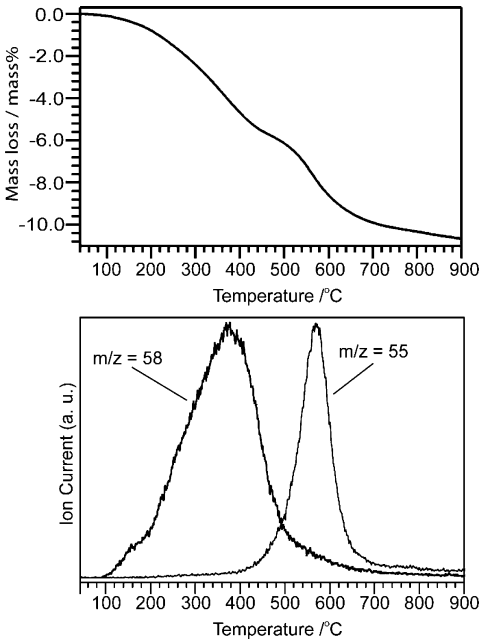

Figure 9. Thermogravimetric curve (top) and mass spectrometric analysis (bottom) of **3(acetone)**. The mass fragments correspond to molecular fragment ($m/z = 58$) of acetone and the representative fragment ($m/z = 55$) of dodecyl alcohol.

the TG-MS data for the sample dried for 48 h are shown in Figure 8. The TG curve of **3(DMSO)** shows a five-step weight loss at around 70, 150, 250, 350, and 550 °C (Figure 8 (top), dotted line). The first weight loss at 70 °C (∼12%) is due to the desorption of DMSO from external or interlayer surface. Other weight losses are also observed for the sample dried for 48 h (Figure 8 (top), solid line). The weight loss at 150 °C corresponds to the desorption of residual DMSO, because the molecular ion ($m/z = 78$) was detected by MS (Figure 8 (bottom)). The third and fourth weight losses are associated with

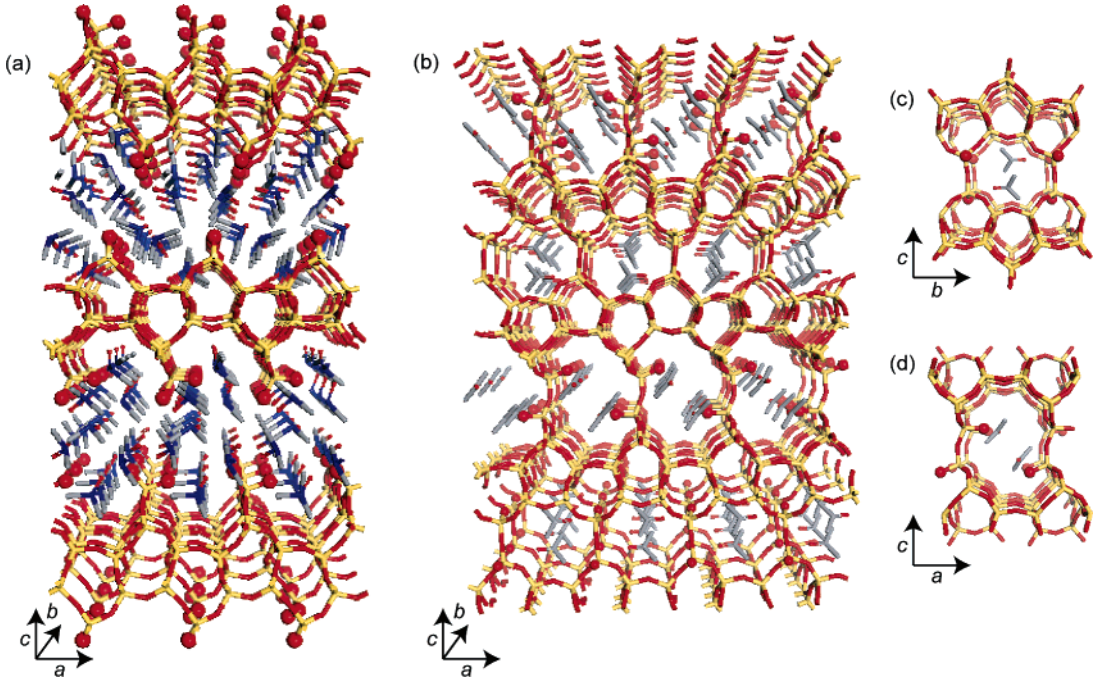

Figure 10. Proposed crystal structural model of **3(DMSO)** and **3(acetone)** as simulated using Discover. Perspective view of (a) **3(DMSO)** and (b) **3(acetone)** along *b* axes. Location of acetone in the cage of **3(acetone)**: (c) view along *a* axis and (d) view along *b* axis, respectively. Color bonding: yellow = Si, red = O, gray = C, blue = S, and red ball = OH.

the thermal decomposition of DMSO. Between 250 and 400 °C, the mass fragment of $[HCS]^+$ ($m/z = 45$) is mainly observed, while the molecular ion ($m/z = 78$) of DMSO is hardly observed. The final weight loss above 450 °C is due to the decomposition of the residual dodecyl alcohol or dodecoxy groups, judging from the representative fragment of dodecyl alcohol ($m/z = 55$) (not shown). The FT-IR spectrum of **3(DMSO)** heated at 550 °C (not shown) exhibits a new band at 3669 cm^{-1}, suggesting that the isolated Si−OH groups were generated upon removal of DMSO molecules. The amount of adsorbed DMSO evaluated from the total weight loss (8.0 wt %) in the range of 250−400 °C was 1.0 molecule per uncondensed Si−OH groups.

Figure 9 shows the TG-MS data for **3(acetone)**. The initial weight loss up to 430 °C is due to the desorption of acetone, judging from the molecular ion ($m/z = 58$) of acetone. The secondary weight loss started from 430 °C is due to the residual dodecyl alcohol or dodecoxy group in the hydrolyzed product, judging from the representative fragment of dodecyl alcohol. The amount of adsorbed acetone, calculated from the weight loss up to 430 °C (6.0 wt %), is 0.7 per Si−OH, being in agreement with the IR data showing that acetone molecules interact with Si−OH groups. In contrast to **3(DMSO)**, **3(acetone)** collapsed upon calcination at 450 °C to form amorphous silica that shows no peaks in the XRD pattern (Figure S5).

Discussion

The silica structures created by silylation of layered silicates depend on the crystal structure of layered silicate, in particular, the configuration of Si−OH (or O^-) groups, as well as the molecular structure of the silylating agent. The silicate layer of octosilicate is schematically shown in Scheme 2A. The O···O distance between confronting Si−OH (or O^-) groups is about 0.23 nm, whereas the distance along the perpendicular direction is much larger (∼0.73 nm). On the basis of the results that one alkoxytrichlorosilane reacted with two Si−OH groups of octosilicate, it is reasonable that silyl groups bridge two confronting silanol groups (designated as 1:2 reaction) (Scheme 2B). The 1:2 reaction with two silanol groups pointing opposite each other (O···O distance of 0.51 nm) to form 3MR should be difficult because of the large O···O distance and the wide Si−O−Si angle (∼219°) that requires the partial restructuring of the siloxane networks of octosilicate. Thus new 5MR are formed on both sides of the silicate layer, resulting in the increase of the layer thickness. The long alkoxy groups of the silylating agent (**1(C_n)**) play a role in inducing the 1:2 reaction and avoiding 1:1 reaction of silylating agents with only one silanol group.[13e,15] However, the direction of Si−OR (or Si−Cl) group on the silicate surface could be random. This may cause slight variations in the local environment of silicate framework, which is responsible for the lowering of the space group symmetry suggested by the XRD pattern and the relatively broad signals in the ^{29}Si MAS NMR spectrum (Figure 3b).

Figure 10 shows the proposed structural models for **3(DMSO)** and **3(acetone)** obtained by hydrolysis of **2(C_{12})**. As shown in Figure 10a, **3(DMSO)** consists of a new layered silica structure containing DMSO molecules between the layers, which is revealed by the much larger *d* value (1.66 nm) than the basal spacing of protonated octosilicate (H−Oct; $d = 0.74$ nm[14g]). The silica structure of **2(C_{12})** is retained, while the geminal Si−OH groups are formed on the interlayer surface. It is noteworthy that **3(DMSO)** possesses a well-ordered local structure, as evidenced by the narrow widths (50−85 Hz) of the Q^2 and Q^4 signals comparable to those of octosilicate. The new layered structure covered with unique geminal $=Si(OH)_2$ (Q^2) surface is expected to be reused as a starting material for further modification, and it may be applicable to unique interlayer adsorption due to the characteristic interlayer environment. The direct evaluation of the amount of interlayer DMSO

is difficult because the product also contains DMSO adsorbed on external surface and H_2O produced by condensation of Si−OH groups. Here, we roughly estimate the amount of interlayer DMSO based on the relationship between the *d* value and the desorbed amount of DMSO. As described before, the *d* value of the product decreased from 1.11 to 0.88 nm (Δd = 0.23 nm) upon desorption of 1.0 molecule of DMSO per one Si−OH group. The Δd value of **3(DMSO)** is 0.81 nm (1.69−0.88 nm), which corresponds to 3.5 molecules per one Si−OH group.

On the other hand, the structure of **3(acetone)** is in marked contrast to that of **3(DMSO)**. The condensation between attached silyl groups was evidenced by ^{29}Si MAS NMR. The attached silyl groups do not form Q^4 units but Q^3 units, indicating that one hydroxyl group per attached group remained uncondensed. It is apparent that the condensation occurred between adjacent layers, because the distance between the grafted silyl groups on the same layer (0.73 nm) is too long for condensation (Scheme 2B). Nevertheless, the *d* value (1.12 nm) is still larger by 0.38 nm than that of H−Oct, which is consistent with the presence of additional SiO_4 units between layers. Figure 10b displays the geometry-optimized model for the structure of **3(acetone)** obtained by using the MD simulation. This model consists of new siloxane rings such as 8MR and 12MR, and Si−OH groups interacting with acetone. A Rietveld refinement was performed on the X-ray powder pattern using this structural model. The final fit obtained between the calculated and observed patterns (Supporting Information, Figure S6) converged to R_{wp} = 0.106. The low quality of the Rietveld refinement could be explained by additional phases (e.g., a remained alcohol phase revealed by TG-MS) and the low-angle peak asymmetry.

The formation process of such silica nanostructures from **2(C*n*)** involves two steps: (1) hydrolysis of the Si−Cl and Si−OR group in the swelling interlayer spaces to form the 2-D silica structure, and (2) silanol condensation between adjacent layers upon desorption of the solvents, forming the 3-D structure. The solvents are crucial for the condensation step. The structure of resulting silica (2-D or 3-D) depended on the kind of solvents (DMSO or acetone). It is known that DMSO molecules are intercalated into various layered silicates due to their ability to form strong hydrogen bonds with silanol groups.[13a,b] In the case of **3(DMSO)**, the presence of DMSO molecules between the layers should prevent the condensation between adjacent layers. Although this 2D structure was very stable in an atmospheric condition, interlayer condensation occurs upon desorption of the DMSO molecules by extending the drying time in vacuo up to 48 h. In the case of **3(acetone)**, interlayer condensation occurred within 2 h of drying in vacuo. This is explained by the high volatility of acetone, and this made it difficult to keep a swelling state of silicate layers. We confirmed that other polar solvents such as 2-butanone, cyclohexanone, and acetonitrile were also available to form 3-D silica structures accommodating each solvent. In addition, when **2(C_{12})** was treated with water in the absence of solvent, pyridine (HCl trap) was adsorbed within 3-D silica structures.

The 3-D silica structure of **3(acetone)** has two characteristic properties. The first is the weak acidity as evidenced by the chemical shift of the carbonyl group of acetone in the ^{13}C CP/MAS NMR spectrum. Purely siliceous mesoporous silica can work as catalysts in several reactions, although the detailed mechanism is still controversial.[27] The other characteristic property is its thermal behavior. The desorption of acetone in **3(acetone)** occurred at around 380 °C (Figure 9), which is much higher than that adsorbed in a protonated zeolite (H−ZSM-5) (∼200 °C).[28] It appears that the acetone molecules are trapped within the 3-D silica frameworks. The simulated model (Figure 10c and d) illustrates that the aperture of the siloxane networks formed by interlayer condensation is slightly narrower (∼0.23 nm)[29] than the molecular length of acetone, because the large aperture along 12MR consists Si−OH groups as an interruption. This nanostructure acts as a nanocapsule trapping the 1−2 molecules of acetone that are hydrogen bonded to surface hydroxyl groups.

After calcination at 450 °C, **3(DMSO)** still retained the ordered structure, whereas **3(acetone)** became amorphous (Figure S5). This difference may arise from the difference in the thermal stability of solvent molecules. The TG-MS spectrum of **3(acetone)** shows the molecular fragment even at high temperature (Figure 9). It is presumable that the silica structure was partly collapsed upon desorption of acetone because of the narrow aperture of the frameworks as compared to the molecular size of acetone. On the other hand, in the case of **3(DMSO)**, the pyrolysis of DMSO was observed during the secondary weight loss, because of the low appearance energy for $CH_3^•$ from DMSO (10.64 eV).[30] This pyrolysis of DMSO proceeds via transformation from a branched molecule to linear fragments, which could run through the silica aperture without the collapse of silica structure. The final silica structure of calcined **3(DMSO)** may be shrunk along the *c*-axis to form a dense silica structure without porosity, because the resulting silica does not adsorb any gases (N_2, Ar, and H_2O).

Conclusion

We have described a new methodology for constructing silica nanostructure based on the silylation of layered silicate octosilicate with alkoxytrichlorosilanes and the subsequent reaction within the interlayers. The silylated product has thicker siloxane layers containing new five-membered siloxane rings bearing Si−Cl and Si−OR groups. This is the first example of the functionalization of layered silicates with Si−Cl groups, which exhibited the high reactivities with alcohol or water. Hydrolysis of both Si−Cl and Si−OR groups by H_2O/DMSO mixture led to the formation of a unique crystalline layered silicate with geminal silanols. Interestingly, the 2-D layers were subsequently transformed to 3-D networks when acetone was used instead of DMSO during hydrolysis. The acetone molecules are trapped within the 3-D structure. Such behavior is promising for the design of zeolite-like materials that encapsulate and stabilize small molecules within the cage even at high temperatures. Furthermore, this 3-D structure contains abundant Si−OH

(27) (a) Iwamoto, M.; Tanaka, Y.; Sawamura, N.; Namba, S. *J. Am. Chem. Soc.* **2003**, *125*, 13032−13033. (b) Yamamoto, T.; Tanaka, T.; Funabiki, T.; Yoshida, S. *J. Phys. Chem. B* **1998**, *102*, 5830−5839. (c) Yamamoto, T.; Tanaka, T.; Inagaki, S.; Funabiki, T.; Yoshida, S. *J. Phys. Chem. B* **1999**, *103*, 6450−6456. (d) Inaki, Y.; Yoshida, H.; Kimura, K.; Inagaki, S.; Fukushima, Y.; Hattori, T. *Phys. Chem. Chem. Phys.* **2000**, *2*, 5293−5297.
(28) Kofke, T. J. G.; Gorte, R. J.; Farneth, W. E. *J. Catal.* **1988**, *114*, 34−45.
(29) The size is measured by considering van der Waals radii of the constructing atoms.
(30) Ruttink, P. J. A.; Burgers, P. C.; Terlouw, J. K. *Chem. Phys. Lett.* **1994**, *229*, 495−498.

groups originated from silylating agents within the silica networks, which is not attained by conventional methods. The present approach can be extended to the use of other layered silicates such as magadiite,[12] RUB-15,[31] and HLS[32] in combination with various silylating agents. Further silylation and hydrolysis of 2-D silica structures such as **3(DMSO)** is also promising for the emergence of a variety of crystalline 2-D and 3-D silica frameworks. We are now focusing on the generation of porosity in the products, which is of particular interest from a technological viewpoint.

Acknowledgment. We thank Professors Y. Sugahara and M. Ogawa (Waseda University) for helpful discussion and Ms. M. Nakagawa for technical discussion. The work was partially supported by a Grant-in-Aid for Center of Excellence (COE) Research "Molecular Nano-Engineering", the 21st Century COE Program "Practical Nano-Chemistry", and Encouraging Development Strategic Research Centers Program "Establishment of Consolidated Research Institute for Advanced Science and Medical Care", MEXT, Japan. D.M. and A.S. are grateful for financial support via a Grant-in-Aid for JSPS Fellows from MEXT.

Supporting Information Available: Si-29 NMR and C-13 NMR spectra of **1(C$_6$)**−**1(C$_{12}$)**; XRD patterns and C-13 CP/MAS NMR spectra of **2(C$_6$)**−**2(C$_{12}$)**; FT-IR and Raman spectra of **3(DMSO)** and **3(acetone)**; XRD patterns of **3(acetone)** calcined at 450 °C; Rietveld refinement pattern of **3(acetone)**; and table giving relative intensity in Si-29 MAS NMR spectra for **2(C$_6$)**−**2(C$_{10}$)**. This material is available free of charge via the Internet at http://pubs.acs.org.

JA042194E

(31) Oberhagemann, U.; Bayat, P.; Marler, B.; Gies, H.; Rius, J. *Angew. Chem., Int. Ed. Engl.* **1996**, *35*, 2869−2872.
(32) (a) Akiyama, Y.; Mizukami, F.; Kiyozumi, Y.; Maeda, K.; Izutsu, H.; Sakaguchi, K. *Angew. Chem., Int. Ed. Engl.* **1999**, *38*, 1420−1422. (b) Ikeda, T.; Akiyama, Y.; Izumi, F.; Kiyozumi, Y.; Mizukami, F.; Kodaira, T. *Chem. Mater.* **2001**, *13*, 1286−1295.